International Journal of Biological Macromolecules 254 (2024) 127922

Contents lists available at ScienceDirect

International Journal of Biological Macromolecules

journal homepage: www.elsevier.com/locate/ijbiomac

CircDYM attenuates microglial apoptosis via CEBPB/ZC3H4 axis in LPS-induced mouse model of depression

Zhongqiu Zhou [a], Qingqing Ye [b], Hui Ren [a], Yuan Zhang [a], Bing Han [a], Honghong Yao [a,c,d], Ying Bai [a,*]

[a] Department of Pharmacology, Jiangsu Provincial Key Laboratory of Critical Care Medicine, School of Medicine, Southeast University, Nanjing, China
[b] Department of Pharmacy, The First Affiliated Hospital of Ningbo University, Ningbo, China
[c] Co-innovation Center of Neuroregeneration, Nantong University, Nantong, China
[d] Institute of Life Sciences, Key Laboratory of Developmental Genes and Human Disease, Southeast University, Nanjing, China

ARTICLE INFO

Keywords:
Microglia
circDYM
CEBPB
ZC3H4
Autophagy
Apoptosis

ABSTRACT

Major depressive disorder (MDD) is a highly prevalent condition and one of the most common psychiatric disorders worldwide. Circular RNA (circRNA) has been increasingly implicated in MDD. However, a comprehensive understanding of circRNA and microglial apoptosis in depression is incomplete. Here, we show that circDYM inhibits microglial apoptosis induced by LPS via CEBPB/ZC3H4 axis. CircDYM prevents the translocation of CEBPB from cytoplasm to the nucleus by binding with CEBPB. Moreover, LPS-induced CEBPB nuclear entry downregulates the expression of ZC3H4, in which promotes autophagy and apoptosis in microglia. Taken together, our findings provide new insights into the relationship between circDYM and microglial apoptosis and shed new light on the function of this novel mechanism in depression-associated complex changes in the brain.

1. Introduction

Major depressive disorder (MDD) is one of the most prevalent psychiatric disorders around the word, and the neuropathogenesis is complex involving intricate gene-environment-psychic interactions [1–5]. There are increasing evidences proving that the neuroinflammation is closely linked with the depression [6–8]. Treatment with lipopolysaccharide (LPS) is widely used in mice to investigate the relationship between neuroinflammation and depression [9–12], and LPS-induced model is one of depression models and has been employed in multiple studies [13–15]. Recent evidence suggests that LPS-induced inflammatory responses in the central nervous system (CNS) act as a vital role in depression [16,17].

Microglia are critical for normal brain function [18–23]. As immune cells in the brain, microglial function is the key factor influencing the progression of depression [24–26]. Multitudinous studies provide evidences that microglia-mediated neuroinflammation acts an essential role in the development of major neurological disorders such as depression [26–30]. Furthermore, dysfunctional microglia can be observed in the hippocampus and other brain regions in LPS-stimulated mice [31,32]. Disruption of microglial function has severe negative effects on CNS development. Thus, the detailed mechanism of the role of microglia in LPS-induced depression remains to be elucidated.

It is extensively known that non-coding RNA acts as a prominent role in the depression pathogenesis [25,33,34]. Various circRNAs have been detected in the brain, suggesting that they play a key role in the proper functioning of the brain [35–37]. The previous study suggested that the loss of circCdr1as caused the dysfunction of synaptic transmission [38]. Moreover, hsa_circRNA_103636 might have the potential to serve as a new class of biomarker for depression [39]. Transplanting gut microbiota from NLRP3 knockout mice to depression mice alleviated depressive-like behaviors via circHIPK2 [40]. Thus, targeting circRNAs to modulate the progression of depression has great potential to become an intervention target for depression.

Therefore, we aimed to demonstrate the associations of circRNAs with LPS-induced depression in mice. Our previous study indicated that the overexpression of circular RNA DYM (circDYM) in the hippocampus significantly ameliorated the LPS-induced depressive-like behavior in mice, which was accompanied by the inhibition of the neuroinflammation induced by microglia activation [31]. However, microglial apoptosis induced in the course of the neuroinflammatory response will further exacerbate the neuroinflammatory response. The effect of

* Corresponding author at: Department of Pharmacology, School of Medicine, Southeast University, Nanjing, China.
E-mail address: yingbai01@seu.edu.cn (Y. Bai).

https://doi.org/10.1016/j.ijbiomac.2023.127922
Received 12 August 2023; Received in revised form 4 November 2023; Accepted 4 November 2023
Available online 7 November 2023

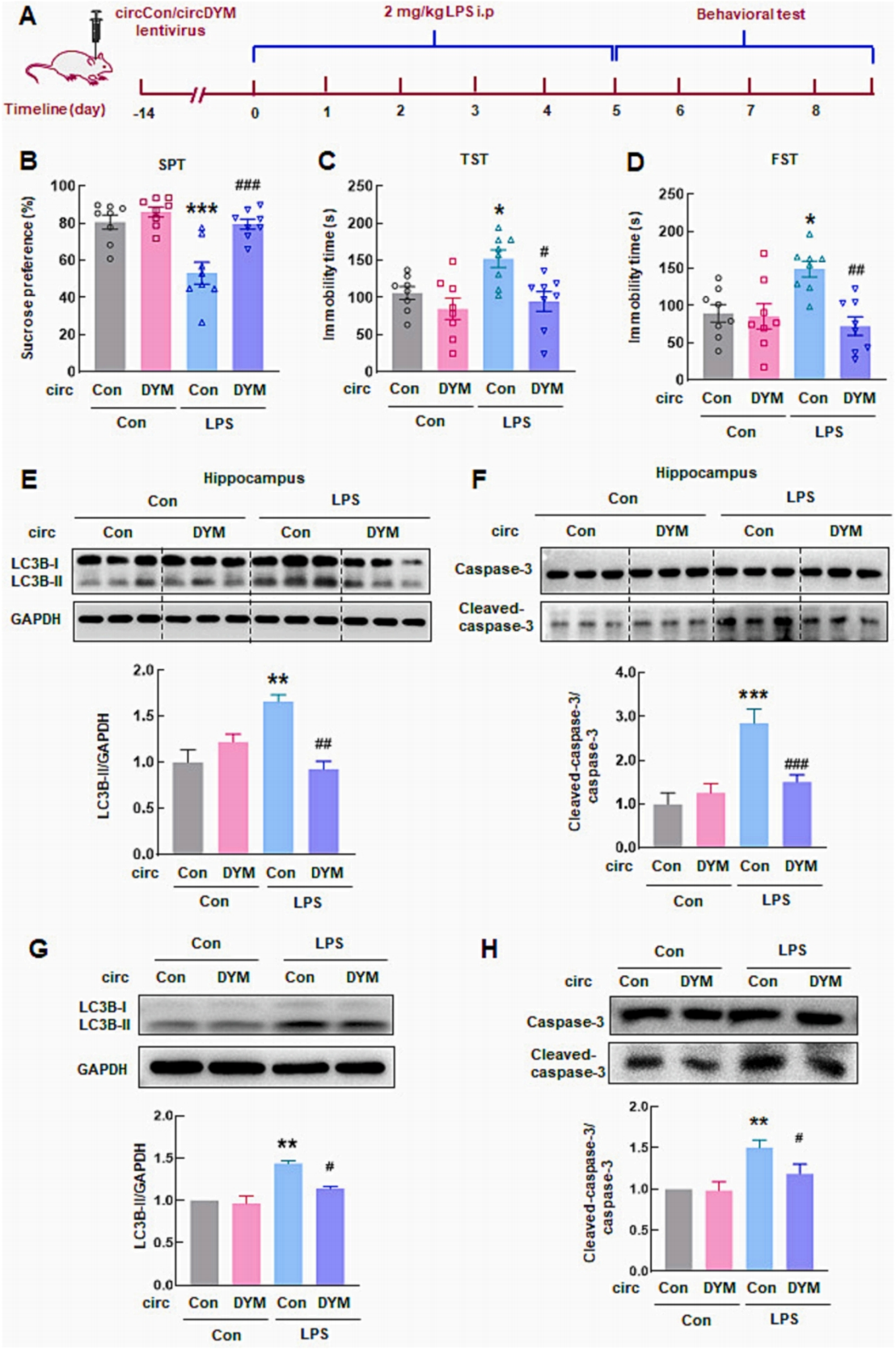

(caption on next page)

Fig. 1. Overexpression of circDYM ameliorates LPS-induced depressive-like behavior. (A) Time course of the experimental procedure in the LPS-induced mouse depressive model. (B—D) Effects of circDYM-GFP lentivirus microinjection on depressive-like behavior in LPS-induced mice. One week after circControl /circDYM lentivirus microinjection, mice were intraperitoneally injected with LPS (2 mg/kg) or saline ($n = 8$ mice/group) for 5 consecutive days. SPT (B), TST (C) and FST (D) were then measured. All data were expressed as mean ± SEM. $^{*}P < 0.05$ and $^{***}P < 0.001$ vs. circControl control group; $^{\#}P < 0.05$ and $^{\#\#}P < 0.01$ and $^{\#\#\#}P < 0.001$ vs. circControl treated with LPS group using two-way ANOVA followed by Holm-Sidak post hoc multiple comparison test. SPT sucrose preference test, TST tail suspension test, FST forced swim test. (E-F) Effects of circDYM overexpression on LC3B-II and cleaved caspase-3 levels in LPS model in the hippocampus. Three representative immunoblots from 6 mice/group were showed. All data were expressed as mean ± SEM. $^{**}P < 0.01$ and $^{***}P < 0.001$ vs. circControl control group; $^{\#\#}P < 0.01$ and $^{\#\#\#}P < 0.001$ vs. circControl treated with LPS group using two-way ANOVA followed by Holm-Sidak post hoc multiple comparison test. (G-H) Transduction with circDYM-GFP lentivirus attenuated LPS-induced LC3B-II and cleaved caspase-3 expression in BV2 cells. Cells were transduced with circControl/circDYM-GFP lentivirus for 24 h and then treated with LPS (100 ng/ml) for another 24 h. All data were presented as mean ± SEM of 3 independent experiments. $^{**}P < 0.01$ vs. circControl control group; $^{\#}P < 0.05$ vs. circControl treated with LPS group using two-way ANOVA followed by Holm-Sidak post hoc multiple comparison test.

circDYM on microglial apoptosis and the mechanisms involved remaines unknown. Our studies were designed to investigate the effects of circDYM on the pathophysiological progression of microglial survival, and provide new theoretical support for the therapy of neuroinflammation-related disorders. The effect of circDYM on microglia suggests a potential therapeutic avenue for inflammation-related brain diseases.

2. Materials and methods

2.1. Reagent

Lipopolysaccharides (L2630), Rapamycin (R0395), and 3-methyladenine (M9281) were all obtained from Sigma-Aldrich.

2.2. Animals

Adult male mice (C57BL/6 J, 25.0–30.0 g, 6–8 weeks old) were purchased from the GemPharmatech Co., Ltd. ZC3H4$^{flox/flox}$ mice (ZC3H4$^{f/f}$, strain ID: T003880) were generated and maintained at GemPharmatech Co., Ltd. Mice were maintained under a constant temperature and 12:12 h light: dark cycle. Food and water were provided ad libitum. The use and care of mice were approved by the Institutional Animal Care and Use Committee (IACUC) of Southeast University.

2.3. circDYM-GFP lentivirus microinjection

All surgical procedures were performed under isoflurane anesthesia (induction at 3 %, maintenance at 1 %–2 %), and mice were placed in a stereotactic frame (RWD, 71000-M) equipped with a heating pad. C57BL/6 J male mice were randomly assigned to different groups. They were microinjected bilaterally with either the circControl-GFP lentivirus or circDYM-GFP lentivirus (Hanbio, 1 μl, 1×10^9 viral genomes/μl) into the hippocampus: 2.06 mm behind the bregma and ± 1.50 mm lateral from the sagittal midline at a depth of 2.00 mm from skull surface.

2.4. Behavioral tests

The mice were brought into the room for testing, and the results were analyzed by an experienced researcher who was blinded to the groups of the mice. All mice need to complete the sucrose preference test (SPT), the tail suspension test (TST), and the forced swim test (FST).

2.5. Cell culture

Cells (BV2) were obtained from the China Center for Type Culture Collection (CCTCC) and maintained in DMEM (Dulbecco's Modified Eagle Medium) containing 10 % fetal bovine serum (FBS) and 1 % penicillin-streptomycin (PS). Cells were further incubated in a humidified incubator (5 % CO_2, 37 °C).

2.6. Western blot (WB) assay

The proteins were first harvested using lysate buffer (Beyotime, P0013B). Samples were separated by sodium dodecyl sulphate-polyacrylamide gel electrophoresis (SDS-PAGE). The proteins were then transferred to polyvinylidene fluoride (PVDF) membranes [41]. The PVDF membranes were blocked with nonfat milk (5 %) and probed with antibodies against LC3B (Sigma, L7543), Caspase-3 (Proteintech, 66,470–2-lg), CEBPB (Proteintech, 66,649–1-lg), GAPDH (Proteintech, 60,004–1-lg), Histone-H3 (Proteintech, 17,168–1-AP), ZC3H4 (Proteintech, 20,041–1-AP), BECN1 (Proteintech, 11,306–1-AP), P62 (Proteintech, 18,420–1-AP), Bcl-xl (Proteintech, 26,967–1-AP), Bax (Proteintech, 50,599–2- lg) overnight at 4 °C. They were then incubated with HRP-conjugated Affinipure goat anti-mouse IgG (H + L) (Proteintech, SA00001–1) and HRP-conjugated Affinipure goat anti-rabbit IgG (H + L) (Proteintech, SA00001–2). Signals were detected by the Tanon 5200 digital image scanner.

2.7. Transduction of microglia with lentivirus

As described in our previous studies [42], BV2 cells were transduced with the circControl-GFP or circDYM-GFP lentivirus. The cells were then gently vortexed, incubated and replaced with fresh medium.

2.8. Immunofluorescence (IF) staining

The BV2 cells were fixed with paraformaldehyde (4 %), and then permeabilized with 0.3 % Triton X-100 in PBS. After blocking with 10 % normal goat serum in 0.3 % TritonX-100, BV2 cells were incubated with a rabbit anti-CEBPB antibody overnight at 4 °C. The cells were then incubated with the AlexaFluor 488-conjugated goat anti-rabbit antibody.

2.9. Target DNA upregulation/deletion using CRISPR/Cas9 plasmids

Following the manufacturer's recommended Santa Cruz® protocol, BV2 cells were transfected with the CRISPR/Cas9 plasmids to upregulate/delete CEBPB and ZC3H4. The efficiency was determined by WB. Briefly, cells were seeded at 2×10^5 cells/well in 2 ml of standard antibiotic-free growth medium and grown to 40–50 % confluency. The plasmid DNA/transfection reagent complex (200 μl), consisting of plasmid DNA (2 μg) and transfection reagent (10 μl), was then added. The BV2 cells were then cultured under standard conditions for 24–72 h prior to the subsequent experiments.

2.10. Flow cytometry and cell sorting

Brain tissue was digested by 2 mg/ml papain (Worthington, LS003119) for 1 h at 37 °C in DMEM. Dispersed cells were filtrated with a 70 μm nylon mesh. The cells were resuspended in 30 % Percoll density gradient (GE Healthcare, 17–0891-09) and centrifuged 900 *g* for 25 min at 25 °C. Next, the cells in bottom were collected. After washing with PBS containing 2 % FBS, the cells were blocked with FcR Blocking

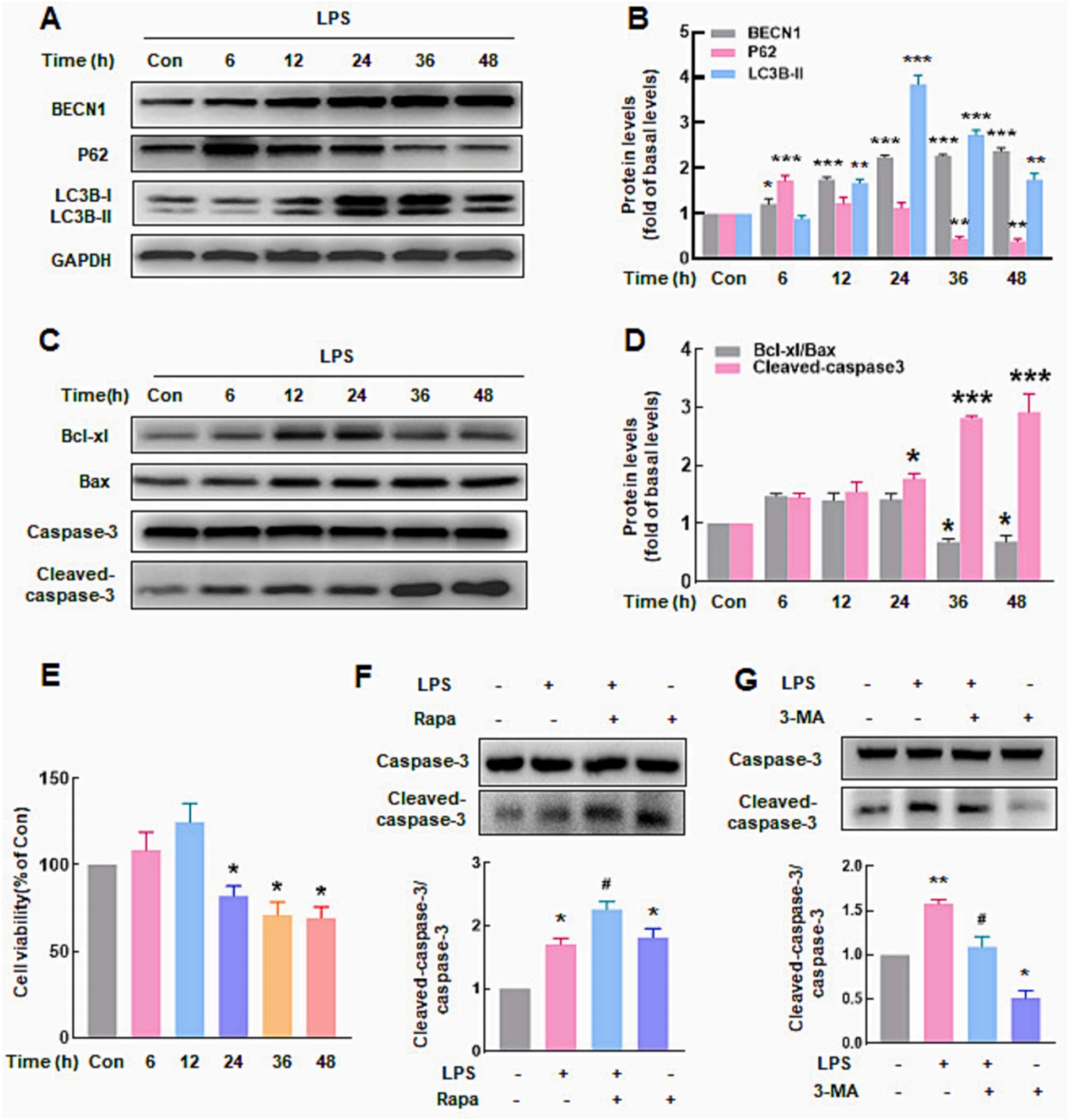

Fig. 2. LPS induces autophagy-mediated apoptosis. (A-B) The expression of BECN1, P62, LC3B in BV2 treated with LPS for 6 h, 12 h, 24 h, 36 h, 48 h. All data were presented as mean ± SEM of 3 independent experiments. $^{*}P < 0.05$, $^{**}P < 0.01$, $^{***}P < 0.001$ vs. control group by one-way ANOVA followed by Holm-Sidak post hoc multiple comparison test. (C—D) The expression of Bcl-xl, Bax, Caspase3 in BV2 treated with LPS for 6 h,12 h,24 h,36 h,48 h. All data were presented as mean ± SEM of 3 independent experiments. $^{*}P < 0.05$, $^{***}P < 0.001$ vs. control group by one-way ANOVA followed by Holm-Sidak post hoc multiple comparison test. (E) CCK8 analysis of BV2 cells survival treatment with LPS for 6 h,12 h,24 h,36 h,48 h. All data were presented as mean ± SEM of 3 independent experiments. $^{*}P < 0.05$ vs. control group using one-way ANOVA followed by Holm-Sidak post hoc multiple comparison test. (F-G) Western blot analysis of the caspase-3 levels after pre-treatment with Rapa or 3-MA in BV2 cells induced by LPS. All data were presented as mean ± SEM of 3 independent experiments. $^{*}P < 0.05$, $^{**}P < 0.01$ vs. control group; $^{\#}P < 0.05$ vs. LPS-treated control group by two-way ANOVA followed by Holm-Sidak post hoc multiple comparison test.

Reagent (Miltenyi Biotec, 130–092-575). Astrocytes, microglial cells, neurons, and endothelial cells were marked by flow cytometry. Cells were stained with FITC anti-mouse/human CD11b antibody (BioLegend, 101,205), PerCp-cy5.5 anti-mouse CD45 antibody (BD Pharmingen, 561,869), PE anti-mouse ACSA-2 (Miltenyi Biotec, 130–116-244), Brilliant Violet 605™ anti-mouse CD31 (BioLegend, 102,427) and, APC anti-mouse NCAM-1/CD56 allophycocyanin MAb (R&D, FAB7820A-100). After staining, the samples were sorted by FACSAria II SORP (BD Biosciences), and the data were analyzed using FlowJo_V10. Samples were gated for ACSA-2^{-}CD11b^{+}CD45^{dim} (microglia), ACSA-2^{+}

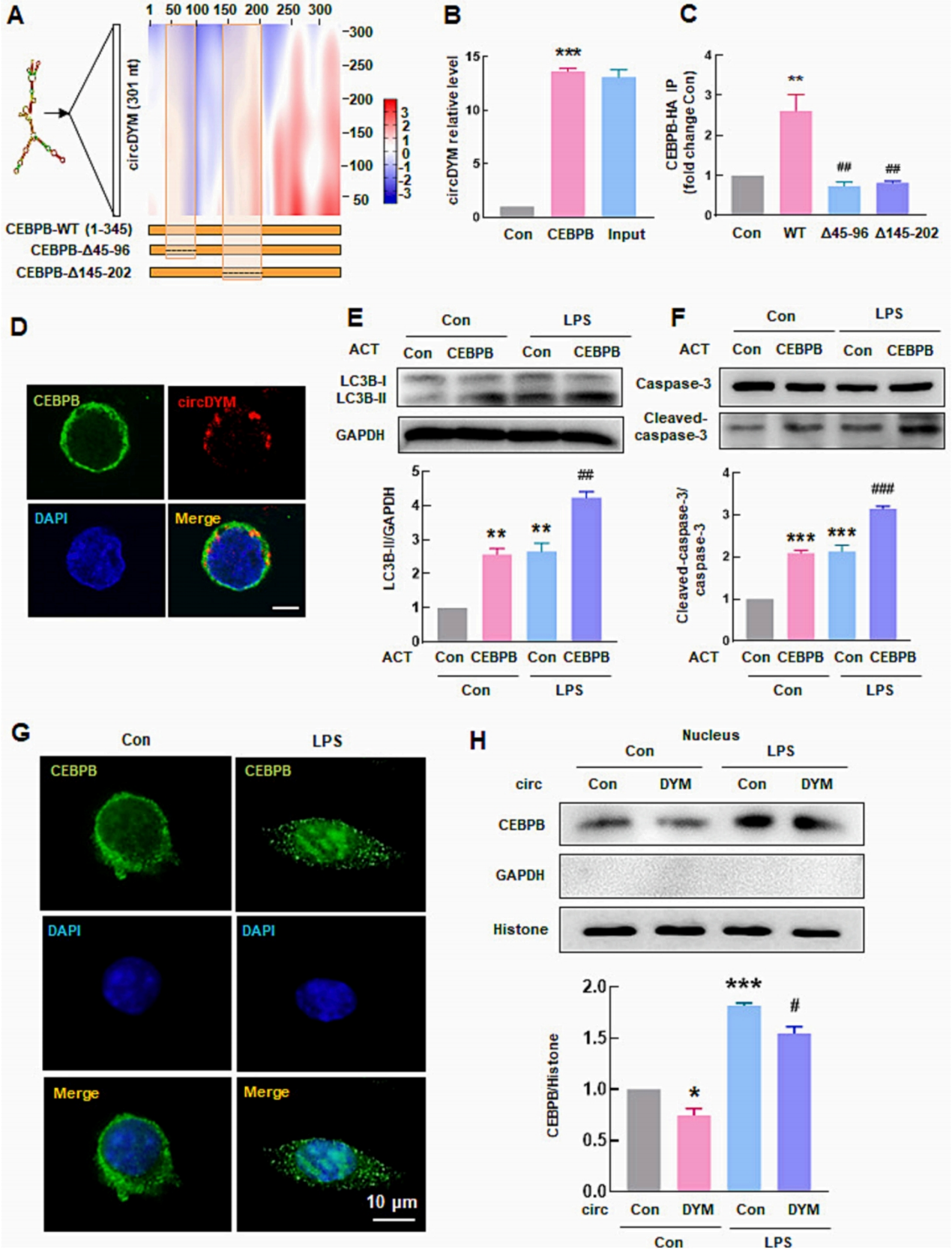

(caption on next page)

Fig. 3. CircDYM attenuates microglial apoptosis induced by LPS through binding to CEBPB. (A) Prediction of the circDYM-CEBPB interaction using the catRAPID algorithm. Schematic of CEBPB with functional protein domains. CEBPB mutants lacking 45 to 96 amino acids (CEBPB Δ45–96) and 145 to 202 amino acids (CEBPB Δ145–202). (B) Relative enrichment of endogenous circDYM in CEBPB RIP was measured by qPCR. Data were presented as mean ± SEM of 3 independent experiments. $^{***}P < 0.001$ vs. control circDYM using Student's *t*-test. (C) Western blot analysis of CEBPB expression in lysates of BV2 cells overexpressing CEBPB or mutant CEBPB (Δ45–96) or mutant CEBPB (Δ145–202) after biotinylated circDYM probe pull-down assay. Data were expressed as mean ± SEM of 3 independent experiments. $^{**}P < 0.01$ vs. control group; $^{\#\#}P < 0.01$ vs. WT group using Student's t-test. (D) Co-localisation of circDYM and CEBPB in the cytoplasm of BV2 cells by FISH analysis. Green: CEBPB; red: circDYM; blue: DAPI. Scale bar: 5 μm. (E-F) Transduction-ACT upregulated CEBPB significantly proposed the increase of LC3B-II and cleaved caspase-3 expression induced by LPS in BV2 cells. All data were presented as mean ± SEM of 3 independent experiments. $^{**}P < 0.01$ and $^{***}P < 0.001$ vs. control-ACT control group; $^{\#\#}P < 0.01$ and $^{\#\#\#}P < 0.001$ vs. control-ACT treated with LPS group by two-way ANOVA followed by Holm-Sidak post hoc multiple comparison test. (G) Distribution of CEBPB in BV2 cells. BV2 cells were subjected to immunocytochemical analysis of CEBPB and DAPI staining of genomic DNA with or without LPS treatment. Scale bar: 10 μm. (H) Western blot analysis nuclear localization of CEBPB in BV2 after circCon or circDYM lentivirus transduction with or without treatment with LPS (100 ng/ml) for 24 h. Purity of subcellular fractions was assessed by Western blotting against specific markers. All data were expressed as mean ± SEM of 3 independent experiments. $^{*}P < 0.05$, $^{***}P < 0.001$ vs. circControl control group; $^{\#}P < 0.05$ vs. circControl LPS group by two-way ANOVA followed by Holm-Sidak post hoc multiple comparison test.

(astrocytes), $CD31^+$ (endothelial cells), and NCAM-1/$CD56^+$ (neurons). The RNeasy®-Micro Kit (QIAGEN, 74004) was used for RNA extraction.

2.11. Quantitative real-time PCR

The total RNA was reversed using a HiScript Q RT SuperMix for qPCR Kit (Vazyme, R123–01). Next, the relative quantification was performed using AceQ qPCR SYBR Green Master Mix (Vazyme, Q141–02). Cycle threshold was determined using the StepOne™ Real-Time PCR instrument.

2.12. Statistical analysis

All data were presented as the mean ± standard error of the mean (SEM). Significance was determined using Student's *t*-test for comparisons of two groups. Multi-groups (three or more) were compared using one/two-way ANOVA. $P < 0.05$ was regarded as statistically significant.

3. Results

3.1. Overexpression of circDYM ameliorates depressive-like behaviors induced by LPS

As described in our previous studies [31] , the expression of circDYM in the hippocampus of mice was markedly decreased induced by LPS. Based on this point, we sought to verify the contribution of circDYM in the hippocampus of depressive mice by microinjecting either the circDYM-GFP lentivirus or the circControl-GFP lentivirus (Fig. 1A). As shown in Fig. 1B, mice treated with LPS preferred sucrose less compared to the control group, and this was significantly meliorated by circDYM overexpression. To further assess the impact of circDYM on depression, two additional behavioral tests were used. In TST (Fig. 1C) and FST (Fig. 1D), the immobility time was significantly longer in LPS group than in control group, which was markedly ameliorated in the group microinjected with circDYM lentivirus. These experiments suggested that overexpression of circDYM by lentivirus contribute to the alleviation of depressive behaviors in mice.

3.2. Overexpression of circDYM inhibits autophagy and apoptosis induced by LPS

Although circDYM has been reported in our previous studies [31], its role in LPS-induced microglial autophagy and survival remained unclear. Therefore, we investigated the effect of LPS on mouse hippocampal microglia to elucidate how LPS affects microglial autophagy and apoptosis. As shown in Fig. 1E, the expression of LC3B-II was markedly increased treated with LPS, and the increasing was ameliorated by circDYM. Furthermore, LPS-mediated upregulation of cleaved caspase-3 was ameliorated in circDYM-injected mice compared with circCon group in the hippocampus (Fig. 1F). Moreover, circDYM significantly ameliorated the increase of LC3B-II and cleaved caspase-3 expression in BV2 cells treated with LPS (Fig. 1G-H). Taken together, the above results indicate that circDYM is involved in the autophagy and apoptosis in microglia induced by LPS.

3.3. LPS induces autophagy-mediated apoptosis

To investigate the relationship between LPS-induced autophagy and apoptosis in microglia, we designed the following experiments. As shown in Fig. 2A-B, BECN1 expression was elevated and LC3B-II production was enhanced in LPS-treated BV2 cells. For the autophagy, P62 functions as a connector that links LC3B with ubiquitin moieties on misfolded proteins. Therefore, autophagy facilitates the elimination of P62 and ubiquitinated proteins. Consistently, P62 expression was downregulated in BV2 cells after treatment with LPS. We next sought to explore the apoptosis in the LPS-treated BV2 cells. As shown in Fig. 2C-D, LPS decreased the Bcl-xl/Bax and increased cleaved caspase-3.

Having determined that LPS induced apoptosis, we next examined viability of LPS-treated cells. As shown in Fig. 2E, exposure to LPS reduced microglial survival. Moreover, cleaved caspase-3 was enhanced by treating with the autophagy inducer rapamycin (Fig. 2F). To further confirm the role of autophagy in LPS-induced apoptosis, BV2 cells were treated with 3-MA, which decreased the level of cleaved caspase-3 (Fig. 2G). Therefore, our findings confirmed that the apoptosis induced by LPS was mediated by autophagy, and the exact mechanism that circDYM inhibits apoptosis by autophagy needs to be elucidated.

3.4. CircDYM attenuates microglial apoptosis induced by LPS through binding to CEBPB

To find this possible mechanism, we, next, used the catRAPID algorithm to explore the interaction of circDYM with CEBPB and found two regions of CEBPB having high interaction capacity with circDYM: 45–96 and 145–202 (Fig. 3A). The binding between CircDYM and CEBPB was determined by RIP assay (Fig. 3B). We also created a circDYM mutant plasmid (45–96, 145–202) in which the circDYM binding region interacting with CEBPB was deleted. Compared to the mutant variant of circDYM, the unmodified circDYM showed stronger binding with CEBPB (Fig. 3C). In addition, fluorescence in FISH analysis demonstrated the co-localization of circDYM and CEBPB in the cytoplasm of microglia (Fig. 3D).

Having established that LPS induced autophagy and apoptosis in microglia, further investigation was undertaken to clarify the integral role of CEBPB in LPS-induced autophagy and apoptosis using the CEBPB-CRISPR activation plasmid (ACT). In Fig. 3E and F, pretreatment of cells with CEBPB-ACT increased LPS-induced autophagy and apoptosis as evidenced by increased levels of LC3B-II and cleaved caspase-3, demonstrating that CEBPB was upstream of autophagy and apoptosis in LPS-treated BV2 cells.

Furthermore, we sought to investigate the CEBPB expression in BV2 cells induced by LPS. CEBPB expression was notably increase in the nucleus in LPS group (Fig. 3G). These facts lead us to conclude that

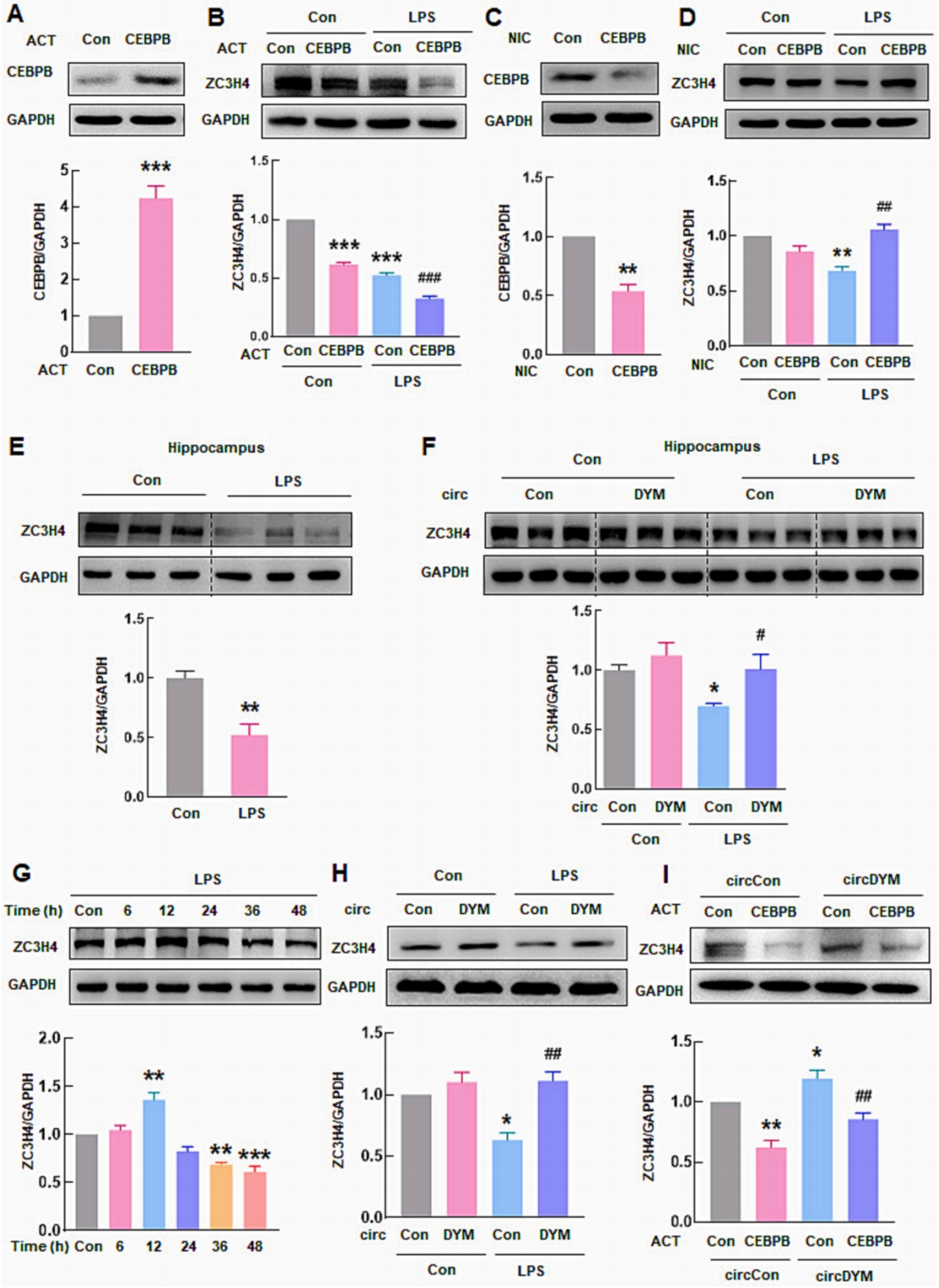

(caption on next page)

Fig. 4. CEBPB regulates the expression of ZC3H4. (A-D) Western blot analysis of the ZC3H4 level induced by LPS in BV2 cells transfected with CEBPB-ACT or CEBPB-NIC. Transduction-ACT upregulated the expression of CEBPB in BV2 cells (A-B). All data were presented as mean ± SEM of 3 independent experiments. $^{***}P < 0.001$ vs. control-ACT control group; $^{\#\#\#}P < 0.001$ vs. control-ACT treated with LPS group by two-way ANOVA followed by Holm-Sidak post hoc multiple comparison test. Transduction-NIC downregulated the expression of CEBPB in BV2 cells (C—D). All data were presented as mean ± SEM of 3 independent experiments. $^{**}P < 0.01$ vs. control-NIC control group; $^{\#\#}P < 0.01$ vs. control-NIC treated with LPS group by two-way ANOVA followed by Holm-Sidak post hoc multiple comparison test. (E) LPS treatment decreased the protein level of ZC3H4 in the hippocampus. All data were presented as mean ± SEM. $^{**}P < 0.01$ vs. control group by Student's *t*-test. (F) Effect of circDYM overexpression on ZC3H4 levels in LPS model in the hippocampus. Three representatives from 6 mice/group were showed. All data were expressed as mean ± SEM. $^{*}P < 0.05$ vs. circControl control group; $^{\#}P < 0.05$ vs. circControl treated with LPS group using two-way ANOVA followed by Holm-Sidak post hoc multiple comparison test. (G) LPS treatment increased ZC3H4 immunoblots in a time-dependent manner. All data were presented as mean ± SEM of 3 independent experiments. $^{**}P < 0.01$, $^{***}P < 0.001$ vs. control group. (H) Western blot analysis of the ZC3H4 level in BV2 after circCon or circDYM lentivirus transduction with or without treatment with LPS (100 ng/ml) for 24 h. All data were presented as mean ± SEM of 3 independent experiments. $^{*}P < 0.05$ vs. control group; $^{\#\#}P < 0.01$ vs. circControl treated with LPS group by two-way ANOVA followed by Holm-Sidak post hoc multiple comparison test. (I) Western blot analysis of the ZC3H4 level in BV2 after co-transfection of CEBPB-ACT and circDYM. All data were presented as mean ± SEM of 3 independent experiments. $^{*}P < 0.05$, $^{**}P < 0.01$ vs. control-ACT group; $^{\#\#}P < 0.01$ vs. control-ACT treated with LPS group using two-way ANOVA followed by Holm-Sidak post hoc multiple comparison test.

CEBPB was transferred from the cytoplasm to the nucleus. As shown in Fig. 3H, overexpression of circDYM decreased the redistribution of CEBPB from the cytoplasm to the nucleus. Collectively, these findings suggest that circDYM regulates LPS-induced the autophagy and apoptosis by binding to CEBPB in microglia.

3.5. CEBPB regulates the expression of ZC3H4

Having established that circDYM regulates CEBPB expression and redistribution, we investigated the role of CEBPB in BV2 cells treated with LPS. It seems clear that transfection with the CEBPB-ACT upregulated the expression of CEBPB in BV2 cells (Fig. 4A). Subsequently, transfection with CEBPB-ACT significantly exacerbated the ZC3H4 expression induced by LPS (Fig. 4B). Contrarily, as shown in Fig. 4C, transfection with the CEBPB-Double Nickase Plasmid (NIC) downregulated the expression of CEBPB in BV2 cells. The LPS-induced reduction of ZC3H4 expression was significantly improved after CEBPB-NIC transfection (Fig. 4D).

Next, an in vivo experiment showed that LPS-treated mice had significantly reduced ZC3H4 expression compared to the control group (Fig. 4E), and these effects were significantly attenuated by circDYM (Fig. 4F). As shown in Fig. 4G, treatment of BV2 cells with LPS resulted in a time-dependent increase in ZC3H4, with peak activation at 12 h and a gradual decrease thereafter. Consistent with these findings, circDYM lentivirus transfection significantly attenuated the LPS-induced decrease in ZC3H4 expression (Fig. 4H). To prove that circDYM is a CEBPB mediator, we co-transfected BV2 cells with CEBPB-ACT and circDYM. The circDYM overexpression enhanced ZC3H4 expression, and this change was significantly attenuated by CEBPB-ACT (Fig. 4I). Thus, these findings suggest circDYM regulates the expression of ZC3H4 by CEBPB.

3.6. ZC3H4 improves microglial apoptosis and promotes the survival by inhibiting autophagy in vitro

Having established that circDYM regulates ZC3H4 expression, we next investigated the role of ZC3H4 in LPS-induced apoptosis. As shown in Fig. 5A-B, transfection with ZC3H4-ACT in BV2 cell contributed to significant amelioration of the increased expression of LC3B-II and cleaved caspase-3. Meanwhile, transfection with the ZC3H4-NIC downregulated the expression of ZC3H4 in BV2 cell and lead to significant aggravation of the increased expression of LC3B-II and cleaved caspase-3 (Fig. 5C-D). To investigate the effects of ZC3H4 on viability, BV2 cells were transfected with ZC3H4-ACT and ZC3H4-NIC. As shown in Fig. 5E, ZC3H4-ACT ameliorated the decrease in cell viability treated with LPS compared to the control, whereas ZC3H4-NIC exacerbated it (Fig. 5F). Together, these data demonstrate that upregulating ZC3H4 promotes microglia survival by inhibiting cell autophagy and, in turn, apoptosis.

3.7. ZC3H4 improves microglial apoptosis and promotes the survival by inhibiting autophagy in vivo

Having shown that ZC3H4, which is involved in the regulation of autophagy, plays a essential role in microglial viability, we aimed to validate the role of microglial ZC3H4 in vivo. Next, we investigated the role of ZC3H4 in LPS-induced microglial apoptosis in vivo. We infused the adeno-associated virus vector AAV9-IBA1-CRE-EGFP-3flag in the hippocampus of $ZC3H4^{f/f}$ mice. Four weeks later, the animals were sacrificed to estimate ZC3H4 mRNA and protein levels. Firstly, we detected the expression of ZC3H4 in microglia, astrocytes, endothelial cells and neurons (Fig. 6A). The results showed a significant downregulation of microglia-derived ZC3H4 compared to astrocyte-, endothelial cell- or neuron-derived ZC3H4 at the mRNA level (Fig. 6B). Next, as shown in Fig. 6C, the $ZC3H4^{f/f}$Iba-1^{Cre} mice showed markedly lower expression of ZC3H4 compared to the $ZC3H4^{f/f}$ mice in protein levels by WB analysis. Additionally, the expression of LC3B-II and cleaved caspase-3 was reduced in LPS-treated $ZC3H4^{f/f}$Iba-1^{Cre} mice (Fig. 6D-G), demonstrating that ZC3H4 plays a indispensable role in microglial viability in vivo.

4. Discussion

Our study shed light on the function of circDYM, which was found to dramatically inhibit microglial apoptosis through autophagy regulation via targeting of CEBPB and subsequent targeting of CEBPB-ZC3H4 (Fig. 6H). These results provide the first evidence that the circDYM/CEBPB/ZC3H4 axis plays a necessary role in microglial apoptosis.

Microglial apoptosis may worsen inflammatory responses and neuronal tissue damage [43]. Past investigations have demonstrated that microglial apoptosis plays a vital role in the pathogenesis of neurotoxicity caused by LPS, which strongly suggests that the inflammatory condition may act as a crucial role in tuning the development and eventual outcome of neural tissue injury [44]. Hence, scientists have concentrated on exploring anti-inflammatory ways for the treatment of microglial apoptosis caused by LPS [45]. In this study, we investigated the molecular mechanisms that are vital for microglial apoptosis. Our results indicated that CEBPB regulated ZC3H4 expression induced by LPS. Intriguing, WB assay revealed that LPS induced a transient increase in ZC3H4 protein levels followed by a decrease in vitro. Therefore, we further investigated the exact mechanisms in this process and discovered that circDYM regulated ZC3H4 protein expression. Our study suggested a new mechanism for ZC3H4 regulation via circDYM/CEBPB axis.

Based on previous research, Kreisel et al. first revealed that chronic unpredictable stress (CUS) led to microglial apoptosis in mice hippocampus whereas the recovery of microglial viability ameliorated the depressive-like behaviors induced by CUS [46]. Then, scientists demonstrated that microglial apoptosis act as a prominent role in depression through various mouse models such as CUS, chronic restraint stress (CRS), and chronic social defeat stress (CSDS) [27,46,47]. Numerous researchers have shown that LPS has been widely used to

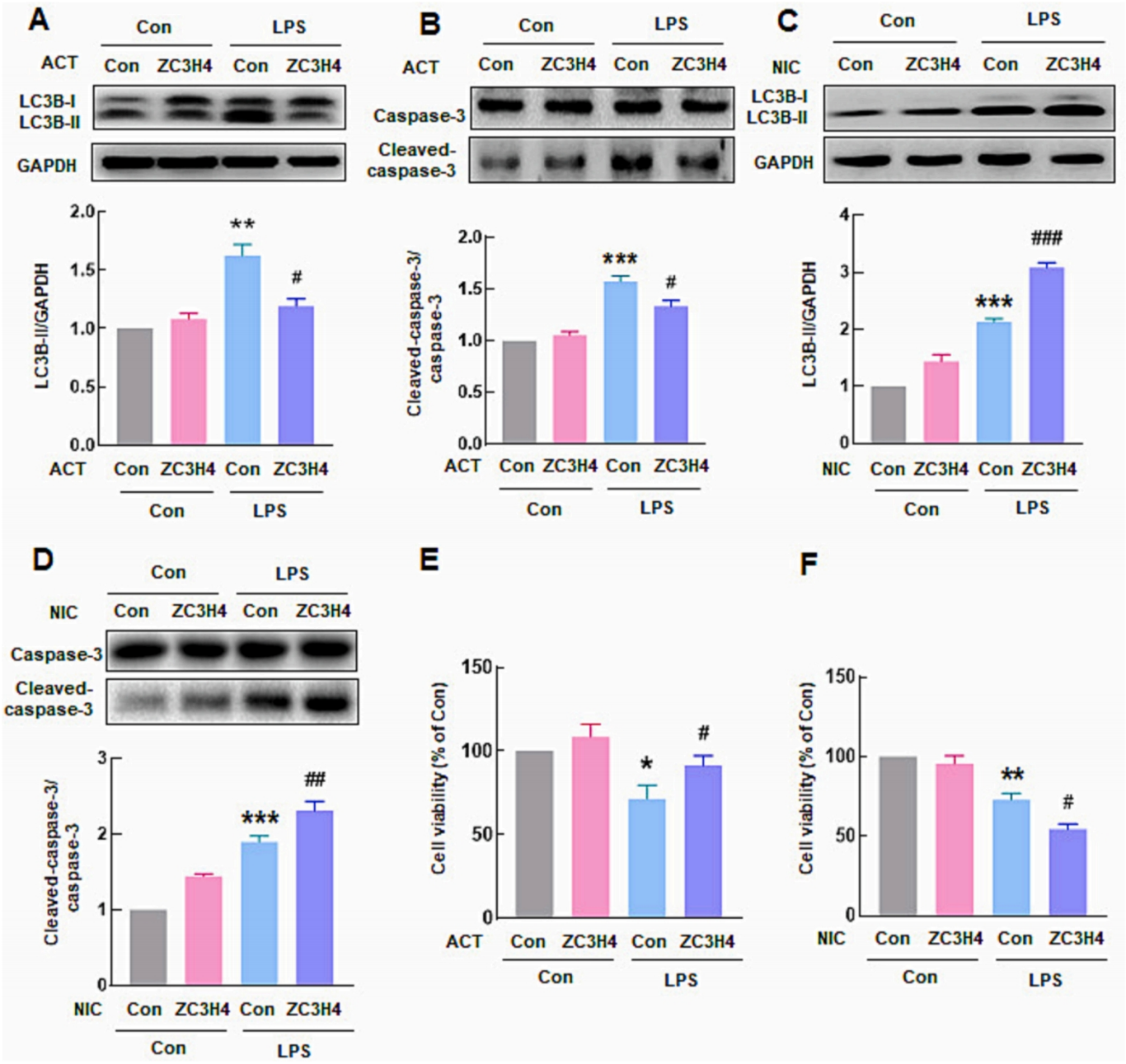

Fig. 5. ZC3H4 improves microglial apoptosis and promotes the survival by inhibiting autophagy in vitro. (A-D) Western blot analysis of LC3B expression and caspase3 level induced by LPS in BV2 cells transfected with ZC3H4-ACT or ZC3H4-NIC. (E-F) CCK8 analysis of BV2 cells survival treatment with LPS transfection with ZC3H4-ACT or ZC3H4-NIC. All data were presented as mean ± SEM of 3 independent experiments. (A-B, E) $^{*}P < 0.05$, $^{**}P < 0.01$, $^{***}P < 0.001$ vs. control-ACT control group; $^{\#}P < 0.05$ vs. control-ACT treated with LPS group using two-way ANOVA followed by Holm-Sidak post hoc multiple comparison test. (C—D, F) $^{**}P < 0.01$, $^{***}P < 0.001$ vs. control-NIC control group; $^{\#}P < 0.05$, $^{\#\#}P < 0.01$, $^{\#\#\#}P < 0.001$ vs. control-NIC treated with LPS group using two-way ANOVA followed by Holm-Sidak post hoc multiple comparison test.

simulate depressive symptoms of mice [48,49]. Consistent with these studies, our results demonstrated that overexpression of circDYM improved depressive-like behaviors induced by LPS and once again strongly emphasized the potential of circDYM as a therapeutic target for depression.

CircRNA, as a kind of special non-coding RNA, exerts significant functions in processes of biology and modulation of gene expression. Numerous studies suggested that they play pivotal roles in neuro-inflammation [50–53]. Garikipati et al. demonstrated that circRNA bound to RNA binding protein and regulated the downstream target gene [54]. In our study, we found that circDYM bound to CEBPB and overexpression of circDYM significantly inhibited CEBPB entering the nucleus, thereby inhibiting the apoptosis of microglia. CEBPB is an important transcription factor that regulates numerous downstream genes. We confirmed that CEBPB represses ZC3H4 expression at the transcriptional level by TF link online prediction software and combined it with previous research [55].

Furthermore, our research approached to determine the significant role of ZC3H4, revealing that ZC3H4 contributes to autophagy and apoptosis. Autophagy acts as a dual role, either promoting or inhibiting cell survival [56–58]. In accordance with our results, LPS decreased ZC3H4 expression while increasing autophagy and apoptosis. Our findings suggested that ZC3H4 exhibits an unexpected function, acting as a survival factor by modulating autophagy and apoptosis. Because of

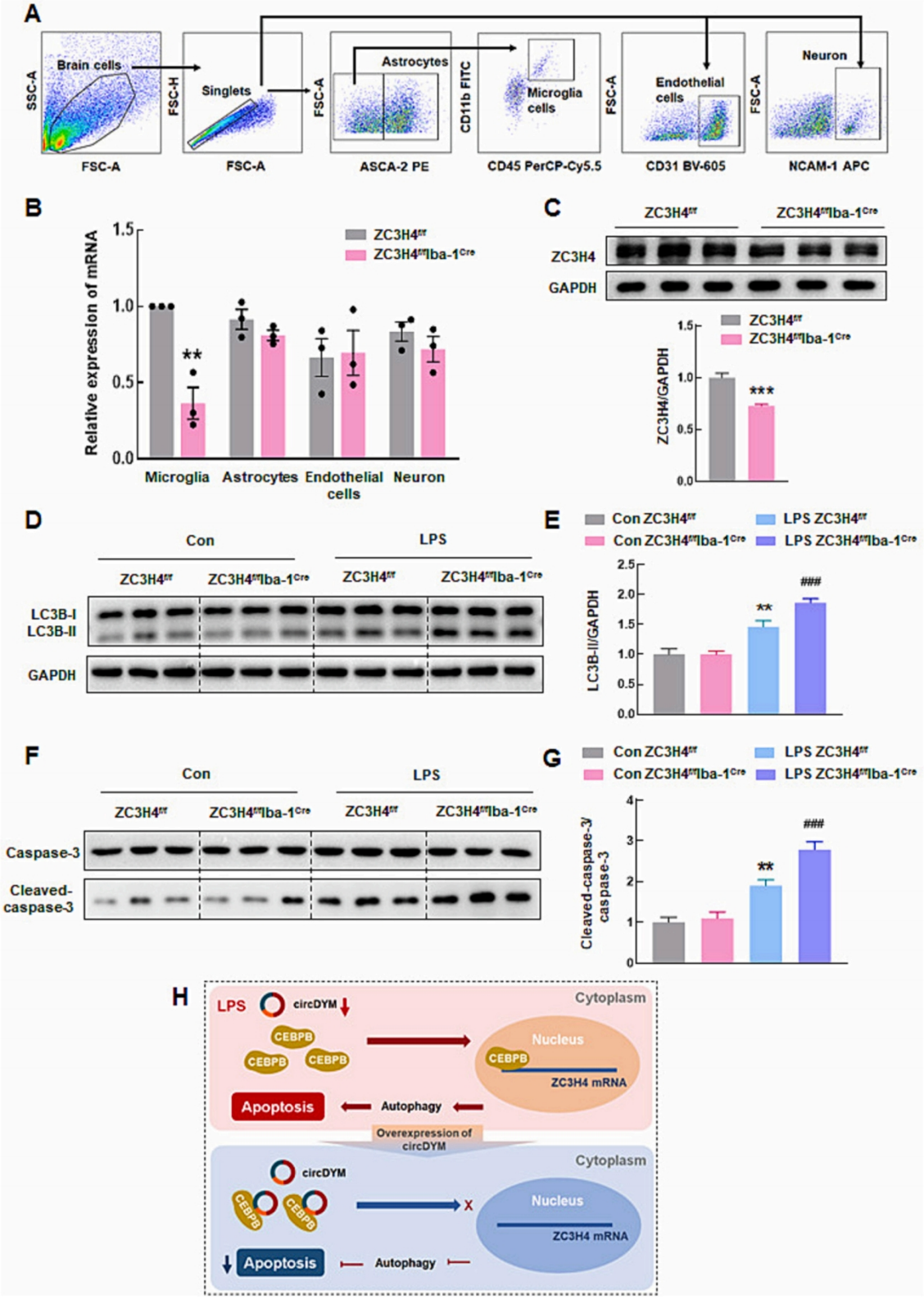

Fig. 6. ZC3H4 improves microglial apoptosis and promotes the survival by inhibiting autophagy in vivo. (A) Schematic of microglia, astrocyte, endothelial cell, and neuron isolation from the hippocampus of ZC3H4$^{f/f}$ and ZC3H4$^{f/f}$Iba-1^{Cre} mice. (B) Relative expression of ZC3H4 in the sorted cells was determined by real-time PCR. $n = 3$ samples for each group. $^{**}P < 0.01$ vs. ZC3H4$^{f/f}$ group. (C) Western blot analysis of ZC3H4 levels in ZC3H4$^{f/f}$Iba-1^{Cre} mice. Three representative immunoblots from 6 mice/group were showed. All data were expressed as mean ± SEM. $^{***}P < 0.001$ vs. ZC3H4$^{f/f}$ group by Student's t-test. (D-G) Effect of ZC3H4$^{f/f}$Iba-1^{Cre} on LC3B (D-E) and caspase-3 (F-G) levels in LPS models in the hippocampus of mice. Three representative immunoblots of 6 mice/group were showed. All data were expressed as mean ± SEM. $^{**}P < 0.01$ vs. ZC3H4$^{f/f}$ group; $^{\#\#\#}P < 0.001$ vs. LPS-treated control group using two-way ANOVA followed by Holm-Sidak post hoc multiple comparison test. (H) Schematic representation of circDYM regulation of microglial function via the CEBPB/ZC3H4 axis.

its potent apoptotic activity, ZC3H4 has been widely regarded as a potential therapeutic target. These results established an innovative molecular relationship between autophagy and apoptosis.

We have shown that circDYM/CEBPB/ZC3H4 regulates the mechanism of LPS-induced microglial apoptosis by lentiviral injection, CRISPR/Cas9 plasmid transfection and combined with the $ZC3H4^{f/f}$Iba-1^{Cre} mice. However, there are still some limitations in our study that should be addressed in future research. First, although the LPS-induced depression model is a classical model, it is undeniable that this model does not represent the pathogenesis of all clinically depressive patients. Moreover, this mechanism involving circDYM/CEBPB/ZC3H4 has not been demonstrated in brain slices or microglia from patients with depression. In addition, we have shown that the upstream pathway by which ZC3H4 regulates microglial apoptosis is circDYM/CEBPB axis, but the exact mechanism by which ZC3H4 inhibits LC3B and caspase-3 levels remains to be explored. Therefore, the tissue or microglia from depressive patients will be examined to confirm that the circDYM/CEBPB/ZC3H4 axis regulates microglial apoptosis, and the transcriptomic analyses will also be performed in the $ZC3H4^{f/f}$Iba-1^{Cre} mice to reveal how ZC3H4 regulates LC3B and caspase-3 levels in future programs.

5. Conclusion

In summary, circDYM attenuates microglial apoptosis via CEBPB/ZC3H4 axis in LPS-induced mouse model of depression. In general, our studies firstly revealed that circDYM regulates microglial apoptosis by targeting the CEBPB/ZC3H4 axis via the autophagy and showed a new role of circDYM in microglial apoptosis. Up-regulation of circDYM may act as an uncharted strategy of therapy for suppression of microglial apoptosis induced by LPS likewise for a broad range of CNS diseases.

CRediT authorship contribution statement

YB, and HHY conceived and designed this study; ZQZ, and QQY performed the experiments, generated animal models; YB, ZQZ, HR, YZ and BH contributed to all aspects of this study, data interpretation, and revised the manuscript for publication.

Funding

None.

Ethics approval and consent to participate

All animal procedures were performed in strict accordance with the Animal Research: Reporting of In Vivo Experiments Guidelines. The care and use of animals were reviewed and approved by the Institutional Animal Care and Use Committee at the Medical School of Southeast University (approval ID: SYXK-2010.4987).

Declaration of competing interest

The authors declare that they have no known competing financial interests or personal relationships that could have appeared to influence the work reported in this paper.

Data availability

The datasets used or analyzed during the current study are available from the corresponding author on reasonable request.

References

[1] C.J. Murray, et al., The state of US health, 1990-2010: burden of diseases, injuries, and risk factors, JAMA 310 (6) (2013) 591–608.
[2] M. Kinjo, et al., Transcranial magnetic stimulation neurophysiology of patients with major depressive disorder: a systematic review and meta-analysis, Psychol. Med. 51 (1) (2021) 1–10.
[3] D.J. Kupfer, E. Frank, M.L. Phillips, Major depressive disorder: new clinical, neurobiological, and treatment perspectives, Lancet 379 (9820) (2012) 1045–1055.
[4] E. Schramm, et al., Review of dysthymia and persistent depressive disorder: history, correlates, and clinical implications, Lancet Psychiatry 7 (9) (2020) 801–812.
[5] M. Fava, K.S. Kendler, Major depressive disorder, Neuron 28 (2) (2000) 335–341.
[6] M. Li, et al., Lentivirus-mediated interleukin-1beta (IL-1beta) knock-down in the hippocampus alleviates lipopolysaccharide (LPS)-induced memory deficits and anxiety- and depression-like behaviors in mice, J. Neuroinflammation 14 (1) (2017) 190.
[7] R.K. Farooq, et al., Role of inflammatory cytokines in depression: focus on interleukin-1beta, Biomed. Rep. 6 (1) (2017) 15–20.
[8] R. Troubat, et al., Neuroinflammation and depression: a review, Eur. J. Neurosci. 53 (1) (2021) 151–171.
[9] B. Zhang, et al., Antidepressant-like effect and mechanism of action of Honokiol on the mouse lipopolysaccharide (LPS) depression model, Molecules 24 (11) (2019).
[10] A.K. Walker, et al., Leucine competes with kynurenine for blood-to-brain transport and prevents lipopolysaccharide-induced depression-like behavior in mice, Mol. Psychiatry 24 (10) (2019) 1523–1532.
[11] Y. Wu, et al., Malva sylvestris extract alleviates the astrogliosis and inflammatory stress in LPS-induced depression mice, J. Neuroimmunol. 336 (2019), 577029.
[12] Y. Tang, et al., Involvement of HECTD1 in LPS-induced astrocyte activation via sigma-1R-JNK/p38-FOXJ2 axis, Cell Biosci. 11 (1) (2021) 62.
[13] P. Cao, et al., Early-life inflammation promotes depressive symptoms in adolescence via microglial engulfment of dendritic spines, Neuron 109 (16) (2021) 2573–2589 e9.
[14] W. Li, et al., Ibrutinib alleviates LPS-induced neuroinflammation and synaptic defects in a mouse model of depression, Brain Behav. Immun. 92 (2021) 10–24.
[15] W. Li, et al., Fluoxetine regulates eEF2 activity (phosphorylation) via HDAC1 inhibitory mechanism in an LPS-induced mouse model of depression, J. Neuroinflammation 18 (1) (2021) 38.
[16] W. Gong, et al., Involvement of the microglial NLRP3 inflammasome in the anti-inflammatory effect of the antidepressant clomipramine, J. Affect. Disord. 254 (2019) 15–25.
[17] R.J. Tynan, et al., A comparative examination of the anti-inflammatory effects of SSRI and SNRI antidepressants on LPS stimulated microglia, Brain Behav. Immun. 26 (3) (2012) 469–479.
[18] G. Piccioni, et al., Targeting microglia-synapse interactions in Alzheimer's disease, Int. J. Mol. Sci. 22 (5) (2021).
[19] M. Prinz, S. Jung, J. Priller, Microglia biology: one century of evolving concepts, Cell 179 (2) (2019) 292–311.
[20] D. Nayak, T.L. Roth, D.B. McGavern, Microglia development and function, Annu. Rev. Immunol. 32 (2014) 367–402.
[21] K. Borst, A.A. Dumas, M. Prinz, Microglia: Immune and non-immune functions, Immunity 54 (10) (2021) 2194–2208.
[22] M. Colonna, O. Butovsky, Microglia function in the central nervous system during health and neurodegeneration, Annu. Rev. Immunol. 35 (2017) 441–468.
[23] S. Hickman, et al., Microglia in neurodegeneration, Nat. Neurosci. 21 (10) (2018) 1359–1369.
[24] S.A. Wolf, H.W. Boddeke, H. Kettenmann, Microglia in physiology and disease, Annu. Rev. Physiol. 79 (2017) 619–643.
[25] Y. Bai, et al., Regulation of glial function by noncoding RNA in central nervous system disease, Neurosci. Bull. 39 (3) (2023) 440–452.
[26] X. Jia, Z. Gao, H. Hu, Microglia in depression: current perspectives, Sci. China Life Sci. 64 (6) (2021) 911–925.
[27] R. Yirmiya, N. Rimmerman, R. Reshef, Depression as a microglial disease, Trends Neurosci. 38 (10) (2015) 637–658.
[28] D.J. Stein, P.J. Naude, M. Berk, Stress, depression, and inflammation: molecular and microglial mechanisms, Biol. Psychiatry 83 (1) (2018) 5–6.
[29] E.S. Wohleb, et al., Integrating neuroimmune systems in the neurobiology of depression, Nat. Rev. Neurosci. 17 (8) (2016) 497–511.
[30] H. Wang, et al., Microglia in depression: an overview of microglia in the pathogenesis and treatment of depression, J. Neuroinflammation 19 (1) (2022) 132.
[31] Y. Zhang, et al., CircDYM ameliorates depressive-like behavior by targeting miR-9 to regulate microglial activation via HSP90 ubiquitination, Mol. Psychiatry 25 (6) (2020) 1175–1190.
[32] B.I. Arioz, et al., Melatonin attenuates LPS-induced acute depressive-like behaviors and microglial NLRP3 inflammasome activation through the SIRT1/Nrf2 pathway, Front. Immunol. 10 (2019) 1511.
[33] N. Liu, et al., Role of non-coding RNA in the pathogenesis of depression, Gene 735 (2020), 144276.
[34] C. He, et al., Identification of microRNA-9 linking the effects of childhood maltreatment on depression using amygdala connectivity, Neuroimage 224 (2021), 117428.
[35] H. Zhang, et al., Total saponins from the leaves of Panax notoginseng inhibit depression on mouse chronic unpredictable mild stress model by regulating circRNA expression, Brain Behav. 8 (11) (2018), e01127.
[36] M. Hanan, H. Soreq, S. Kadener, CircRNAs in the brain, RNA Biol. 14 (8) (2017) 1028–1034.

[37] Y. Bai, et al., Circular RNA DLGAP4 ameliorates ischemic stroke outcomes by targeting miR-143 to regulate endothelial-mesenchymal transition associated with blood-brain barrier integrity, J. Neurosci. 38 (1) (2018) 32–50.
[38] M. Piwecka, et al., Loss of a mammalian circular RNA locus causes miRNA deregulation and affects brain function, Science 357 (6357) (2017).
[39] X. Cui, et al., hsa_circRNA_103636: potential novel diagnostic and therapeutic biomarker in major depressive disorder, Biomark. Med. 10 (9) (2016) 943–952.
[40] Y. Zhang, et al., Gut microbiota from NLRP3-deficient mice ameliorates depressive-like behaviors by regulating astrocyte dysfunction via circHIPK2, Microbiome 7 (1) (2019) 116.
[41] Y. Zhang, et al., Involvement of PUMA in pericyte migration induced by methamphetamine, Exp. Cell Res. (2017).
[42] R. Huang, et al., Circular RNA HIPK2 regulates astrocyte activation via cooperation of autophagy and ER stress by targeting MIR124-2HG, Autophagy 13 (10) (2017) 1722–1741.
[43] R. Lv, et al., Polydatin attenuates spinal cord injury in rats by inhibiting oxidative stress and microglia apoptosis via Nrf2/HO-1 pathway, Life Sci. 217 (2019) 119–127.
[44] T. Muhammad, et al., Hesperetin, a citrus flavonoid, attenuates LPS-induced neuroinflammation, apoptosis and memory impairments by modulating TLR4/NF-kappaB signaling, Nutrients 11 (3) (2019).
[45] C. Li, et al., TREM2 inhibits inflammatory responses in mouse microglia by suppressing the PI3K/NF-kappaB signaling, Cell Biol. Int. 43 (4) (2019) 360–372.
[46] T. Kreisel, et al., Dynamic microglial alterations underlie stress-induced depressive-like behavior and suppressed neurogenesis, Mol. Psychiatry 19 (6) (2014) 699–709.
[47] L. Tong, et al., Microglia loss contributes to the development of major depression induced by different types of chronic stresses, Neurochem. Res. 42 (10) (2017) 2698–2711.
[48] X. Zhao, et al., Behavioral, inflammatory and neurochemical disturbances in LPS and UCMS-induced mouse models of depression, Behav. Brain Res. 364 (2019) 494–502.
[49] T. Ali, et al., Melatonin prevents neuroinflammation and relieves depression by attenuating autophagy impairment through FOXO3a regulation, J. Pineal Res. 69 (2) (2020), e12667.
[50] S. Zhou, et al., A new perspective on depression and neuroinflammation: non-coding RNA, J. Psychiatr. Res. 148 (2022) 293–306.
[51] L. Shen, et al., Non-coding RNA and neuroinflammation: implications for the therapy of stroke, Stroke Vasc. Neurol. 4 (2) (2019) 96–98.
[52] R. Huang, et al., Overexpressing circ_0000831 is sufficient to inhibit neuroinflammation and vertigo in cerebral ischemia through a miR-16-5p-dependent mechanism, Exp. Neurol. 353 (2022), 114047.
[53] M.J. Millan, Linking deregulation of non-coding RNA to the core pathophysiology of Alzheimer's disease: an integrative review, Prog. Neurobiol. 156 (2017) 1–68.
[54] V.N.S. Garikipati, et al., Circular RNA CircFndc3b modulates cardiac repair after myocardial infarction via FUS/VEGF-A axis, Nat. Commun. 10 (1) (2019) 4317.
[55] S.H. Yu, et al., JMJD3 facilitates C/EBPbeta-centered transcriptional program to exert oncorepressor activity in AML, Nat. Commun. 9 (1) (2018) 3369.
[56] N. Mizushima, M. Komatsu, Autophagy: renovation of cells and tissues, Cell 147 (4) (2011) 728–741.
[57] A.V. Onorati, et al., Targeting autophagy in cancer, Cancer 124 (16) (2018) 3307–3318.
[58] K.R. Parzych, D.J. Klionsky, An overview of autophagy: morphology, mechanism, and regulation, Antioxid. Redox Signal. 20 (3) (2014) 460–473.